Histol Histopathol (2019) 34: 257-264

http://www.hh.um.es

Histology and Histopathology

From Cell Biology to Tissue Engineering

Double immunofluorescence labeling for CD31 and CD105 as a marker for polyether polyurethane-induced angiogenesis in mice

Camila Couto Figueiredo[1], Núbia Braga Pereira[1], Luciana Xavier Pereira[2], Laser Antônio Machado Oliveira[3], Paula Peixoto Campos[1], Silvia Passos Andrade[4] and Luciana Moro[1]

[1]Departament of General Pathology, Universidade Federal de Minas Gerais, [2]Universidade Federal de Alagoas, Campus Arapiraca, [3]Departament of Biological Science, Universidade Federal de Ouro Preto and [4]Departament of Physiology and Biophysics, Universidade Federal de Minas Gerais, Brazil

Summary. A crucial component of the integration between foreign implants and the host is angiogenesis. However, to date, none of the available techniques and/or endothelial markers employed to assess angiogenesis in the implant/host interface seems to be able to highlight vascular structures convincingly. In the present study we investigated and compared the expression of two endothelial cell markers: platelet endothelial cell adhesion molecule (PECAM-1) (CD31) and endoglin (CD105) using immunohistochemistry (IHC) and immunofluorescence (IF) to identify and quantify newly formed blood vessels in subcutaneous implants of polyether-polyurethane sponge of formalin-fixed paraffin-embedded tissue. At day 14 post implantation the discs of the synthetic matrix were removed and processed for histological and morphometric analysis. In IHC staining for CD31 antibody the number of vessels was 2.27±0.69 and 5.25±0.46 for CD105. In IF for CD31 the number of vessels was 15.36±1.295 and 10.54±0.8213 for CD105. The level of cross-reaction was lesser in IF images compared with IHC images. Co-localization of CD31/CD105 using confocal images showed positive correlation (Pearson's co-relation and Manders' equation). The double labeling for blood vessels using the IF technique for CD31/CD105 may be an important tool for evaluation of angiogenesis in biomaterial/host integration.

Offprint requests to: Núbia Braga Pereira, Department of Pathology, Biological Sciences Institute, Universidade Federal de Minas Gerais, Av. Antônio Carlos 6627, Pampulha, Belo Horizonte, Minas Gerais, Brazil, CEP 31270-901. e-mail: nubiologicas@gmail.com

DOI: 10.14670/HH-18-038

Key words: Immunohistochemistry, Immunofluorescence, Sponge implant, Confocal microscopy

Introduction

Biomaterials have been extensively employed to repair and/or to replace biological tissues in both human and animals. It is central that such materials allow colonization of the host tissue into the implanted scaffold to rebuild functionality. Biocompatibility and integration of the implanted foreign body depend on a number of factors including the arrival of inflammatory cells and subsequent formation of a fibrovascular tissue (Mendes et al., 2007; Socarrás et al., 2014; Andrade and Ferreira, 2016). A crucial component of the integration between foreign implants and the host is angiogenesis (the development of new blood vessels) which is, in turn, essential in sustaining the organized growth of host tissue into the implant. The endothelium from distinct vascular beds displays a high-degree of phenotypic heterogeneity not only between organs, but also within the different pre-existing vascular beds, and within newly formed vasculatures (McCarthy et al., 1991; Fox, 2009). This poses difficulty in finding common reliable markers for distinct vascular beds. The majority of the studies have highlighted the endothelium using immunohistochemistry and more specific endothelial markers (CD31, CD105) which are present on most capillaries and are reliable epitopes for immunostaining in routinely handled formalin fixed paraffin-embedded tissues (Fox, 2009). In an attempt to identify suitable markers for newly formed blood vessels within and

around the scaffold microenvironment, immunohistochemistry for specific and non-specific vascular markers (von Willebrand factor- vWF, endomucin, platelet endothelial cell adhesion molecule-1 -CD31 and MECA-32) have been used (Van Amerongen et al., 2002). It was found that collagen IV, but not CD31, was the best vascular marker in the subcutaneous collagen type-1 disc model (Van Amerongen et al., 2002). However, collagen IV is present on many non-endothelial elements (Fox, 2009). The unique characteristics of the implanted biomaterial may pose additional difficulty in identifying reliable vascular markers to be used in the assessment of blood vessels in the interface implant/host tissue, as they may differ widely depending on the nature of the biomaterial and the site of implantation. Furthermore, although immunohistochemical staining procedure is one of the pillars of modern diagnostic pathology and a fundamental research tool in both pathology and translational research, its results for some markers present limitations such as background and poor signal (Robertson et al., 2008). These limitations (non-specific background staining, poor signal) apply particularly to different types of biomaterials. There is, thus, the need to establish new methodologies to overcome the drawbacks of current techniques used to identify and quantify blood vessels in the scaffold microenvironment. In this study, we chose to compare immunohistochemical and immunofluorescent staining for the most specific and sensitive endothelial markers currently available, CD31 and CD105, as a possibility to identify and quantify angiogenesis induced by subcutaneous synthetic polyether-polyurethane in mice. This synthetic matrix has been used as the implanted scaffold to analyze the interaction between the host and the foreign body in rodents and to characterize the components of the fibrovascular tissue. To our knowledge, this type of investigation has not been carried out and may reveal a new approach to study angiogenesis in implant scaffold microenvironment.

Materials and methods

Preparation of sponge discs

The present study was approved by the *Comitê de Ética em Experimentação Animal* (CEUA) of the Universidade Federal de Minas Gerais (UFMG) (process number 447/2015). Sponge discs of Polyether-polyurethane sponge (Vitafoam Ltd., Manchester, UK), 6 mm thick, and 11 mm diameter were soaked overnight in ethanol (70% v/v) and boiled in distilled water for 15 min before implantation.

Animals and sponge implantation

Twenty-one Swiss mice were anesthetized with xylazine/ketamine (1 mg/kg, Syntec of Brazil) and trichotomy was performed of the dorsal skin. A dorsal midline incision (1 cm) was performed and the sponge discs were aseptically implanted into subcutaneous tissue. The incision was sutured with n5 silk thread. Fourteen days post implantation the animals were euthanized and the sponge discs were carefully dissected from adherent tissue and removed. The sponge implant was fixed in 10% buffered formalin (pH 7.4), processed for paraffin embedding and for light microscopic studies.

Tissue samples and microscopic analysis

Twenty one formalin-fixed paraffin-embedded (FFPE) sections 4μm thick of implant samples were stained by hematoxylin and eosin (HE) and analyzed for characterization of vascular infiltration. Posteriorly, seven sponge sections were submitted to immunohistochemistry and immunofluorescence.

Immunohistochemistry (IHC)

Formalin-fixed paraffin-embedded (FFPE) sections 4-μm thick were submitted to Immunohistochemistry. Briefly, sections were dewaxed, hydrated and antigen retrieval was performed using citric acid pH 6.0. The endogenous peroxidase was blocked with peroxidase/methanol (1:1) for 30 minutes. Primary antibodies incubation (Table 1) was performed (25ºC). The binding was visualized using a polymer-based system and the revelation was performed with diaminobenzidine (DAB) as chromogen. A negative control without primary antibody was included. The sections were counterstained with hematoxylin, dehydrated, and mounted. Images were captured using light microscopy (Olympus BX-640) and digitized using a JVC TK-1270/JCB micro-camera with a 20x objective.

Table 1. Antibodies used for HRP Immunolabeling.

Primary antibody	Host	Dilution	Antigen retrieval	Manufacturer
Anti-CD31*	Rat Monoclonal	1:50 and 1:100	Water bath (90 min,) or pressure cooker (8 min.)	Santa Cruz Biotechinology®, inc
Anti-CD105*	Rabbit Polyclonal	1:100	Water bath (90 min.) or pressure cooker (8 min.)	ABCAM (ab107595)

* Both antibodies were tested with different visualization systems such as ARK Animal Research kit Peroxidase (Dako cytomation), NovoLink Polymer (Leica) and LSAB+System-HRP (Dako cytomation) according manufactures' instructions.

Immunofluorescence and confocal analysis

FFPE sponge sections (4 μm) were dewaxed in xylene, hydrated and incubated with PBS containing 0.2% Triton X-100 (Sigma-Aldrich) for 20 minutes. The antigen retrieval was performed according to manufactures' instructions (without antigen retrieval or proteinase K for 5-10 minutes). The sections were blocked in PBS containing 5% bovine serum albumin (BSA) (Sigma-Life Science, USA) for 2 hours. The sponge sections were then incubated with primary antibodies (either CD31/CD105 double stain, with CD163 or anti-fibroblast) (Table 2) overnight at 4°C. Subsequently, sections were rinsed in PBS and incubated with Alexa Flour 488 and/or 555 conjugated secondary antibodies (Table 2) for 1 hour at room temperature, washed in PBS, then incubated with Hoechst (1:10000) at 37°C for 30 minutes and then mounted with glycerol. The negative control was included in all reactions by omitting primary antibodies. Images were captured using a Zeiss 5 Live confocal (Carl Zeiss, Jena, Germany) microscope with a 20x and 40x objective lens. The samples were excited at 532 nm to detect Alexa fluor 555 staining, at 505-550 to detect Alexa Fluor 488 and at 405 nm to detect the nuclear staining with Hoechst. The microscopic data shown in this work was obtained using the microscopes and equipment in the *Centro de Aquisição e Processamento de Imagens* (CAPI-ICB/UFMG).

Quantification of co-localization of two antigens

After digitalization, the images were analyzed using Zeiss program. The co-localization index of CD31 and CD105 was determined through Pearson's co-relation and Manders' analysis (Manders et al., 1993). Mander's co-localization coefficients were calculated to predict the contribution of each antigen (CD31 and CD105) to the areas with co-localization, using the following equations:

$$M_{red} = \frac{\sum_i R_i coloc;}{\sum_i R_i} M_{green} = \frac{\sum_i R_i coloc;}{\sum_i G_i}$$

M red is the totality of intensities of red pixels that have a green component divided by the sum total of red intensities.

Background correction in manual mode was determined and kept consistent for all images that were compared. Serial optical sections were collected for three-dimensional reconstruction to confirm co-localization of CD31 and CD105 in many blood vessels.

Number of blood vessels

The number of vessels was performed using five fields of 7 samples that were counted using sections submitted to HE, immunofluorescence and immunohistochemistry techniques. HE is considered as a control. Under immunofluorescence and immunohistochemistry techniques the blood vessels were counted considering at least one marked cell. The quantification was carried out under a 20x objective. The mean and respective standard errors and coefficients of variation were calculated.

Statistical analysis

Results are presented as mean ± standard deviation. Comparisons between all groups were carried out using one-way analysis of variance (ANOVA) and differences between groups were assessed using Newman-Keuls (parametric data). When the group distribution showed no normal distribution (nonparametric) Kruskal Wallis test and Dunn posttest were applied. A $p<0.05$ was considered statistically significant.

Results

Tissue samples and microscopic analyses

Under light microscopy, the histological sections of the sponge implants contained an organized granulation tissue consisting of fibroblasts, inflammatory infiltrate and large amount of blood vessels embedded in an extracellular matrix (Fig. 1).

Immunohistochemistry (IHC) analysis

Immunohistochemistry was performed using the monoclonal antibody clone CD31 and the polyclonal antibody clone CD105. The labeling for the primary antibodies (CD31 and CD105) did not show uniformity (Fig. 2). We observed that some blood vessels had no labeling and others showed few endothelial cells mildly labeled in the same section for both antibodies (pressure cooker as antigenic recovery).

Immunofluorescence and confocal analysis of blood vessels

Our results showed that using double labeling for CD31 and CD105 was more homogeneous and marked

Table 2. Antibodies used for the immunofluorescence study.

Primary antibody/Manufacturer	Dilution	Secundary Antibody/Manufacturer
Anti-CD31/Santa Cruz Biotechinology®, inc (Texas, USA)	1:25	Alexa Flour® 555 anti-rat IgG antibody/Life technologies™ (California, USA)
Anti-CD105/ABCAM (Cambridge, UK)	1:100	Alexa Flour® 488 goat anti-rabbit IgG antibody/Life technologies™ (California, USA)

more vessels, without nonspecific labeling (Fig. 3). No type of antigenic recovery for both primary antibodies CD31/CD105 was used. The best dilution was 1:25 to CD31 and 1:100 to CD105. CD31 monoclonal antibody showed higher fluorescence intensity when compared to CD105 polyclonal antibody. To visualize the co-localization of CD31 and CD105 and for further confirmation of distribution of these two proteins in the vascular endothelium we acquired confocal images of tissue sections (immunostained with two fluorophore mixture simultaneously) (Fig. 4). There was a positive co-localization of CD31 with CD105. However, this correlation was low in some samples analyzed (Table 3). Additionally, three-dimensional reconstruction of serial confocal immunofluorescence images (Fig. 3B) confirmed co-localization of CD31 and CD105 in many blood vessels.

Number of blood vessels using IHC and confocal immunofluorescence

After histopathological characterization of vascular neoformation, sections marked with immunohisto-chemistry and immunofluorescence were analyzed

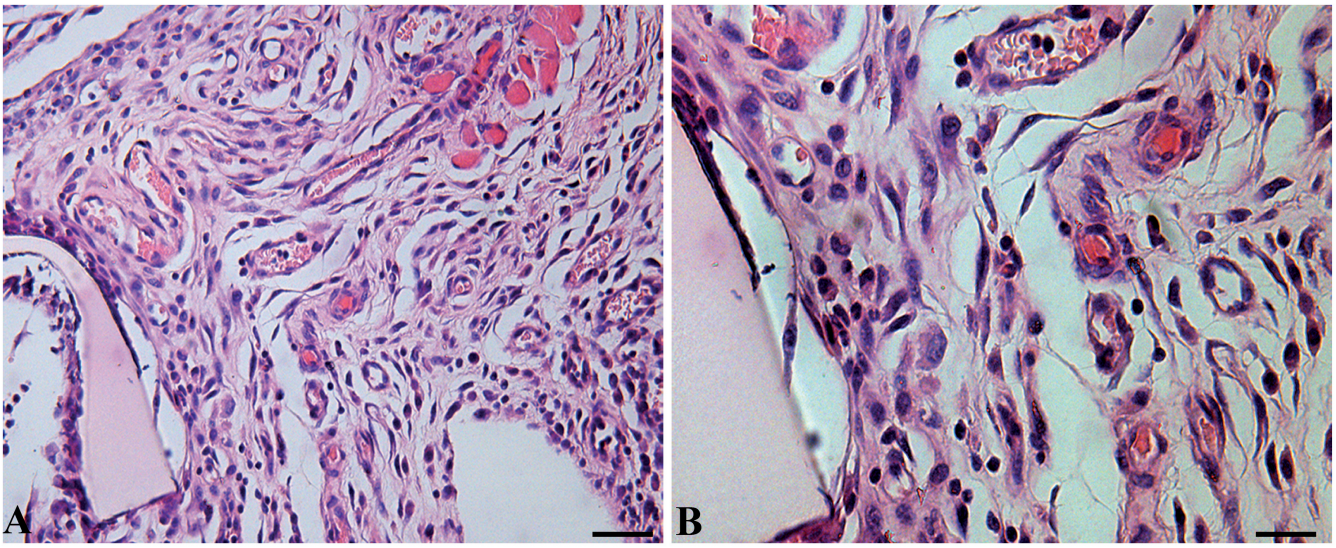

Fig. 1. Representative histological sections of 14-day old subcutaneous implant (H&E). **A.** The fibrovascular tissue induced by the synthetic matrix is composed of inflammatory cells, spindle-shaped fibroblast- like-cells. **B.** Same field in higher magnification. Triangle shapes, *sponge matrix; arrows, blood vessels. Scale bars: 50 μm.

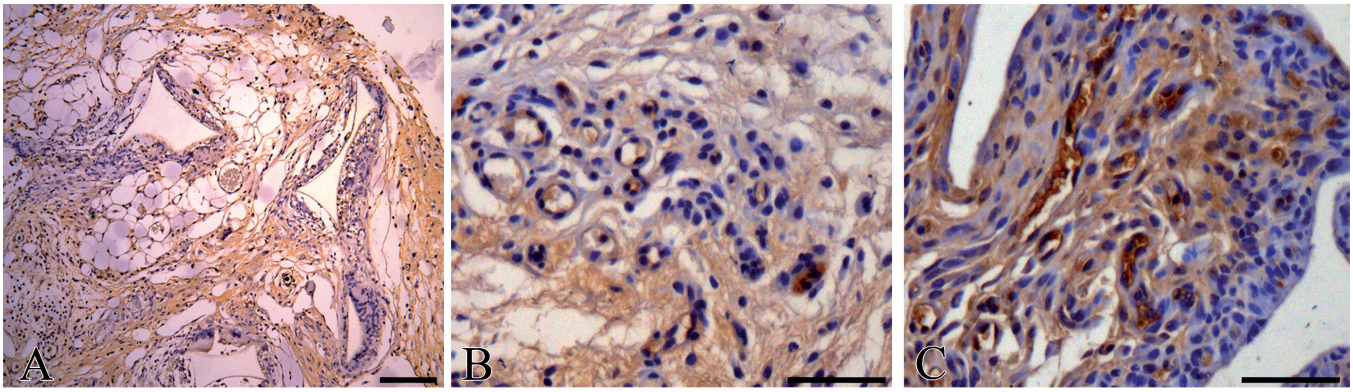

Fig. 2. Representative micrographs of 14-day old implant sections under immunohistochemistry technique. **A.** Negative control. **B, C.** CD31 and CD105 immunostained sections showing newly formed vascular structures within a diffuse, not uniform strong background (pressure cooker as antigenic recovery). Counter-stained with hematoxylin. Scale bars: 50 μm.

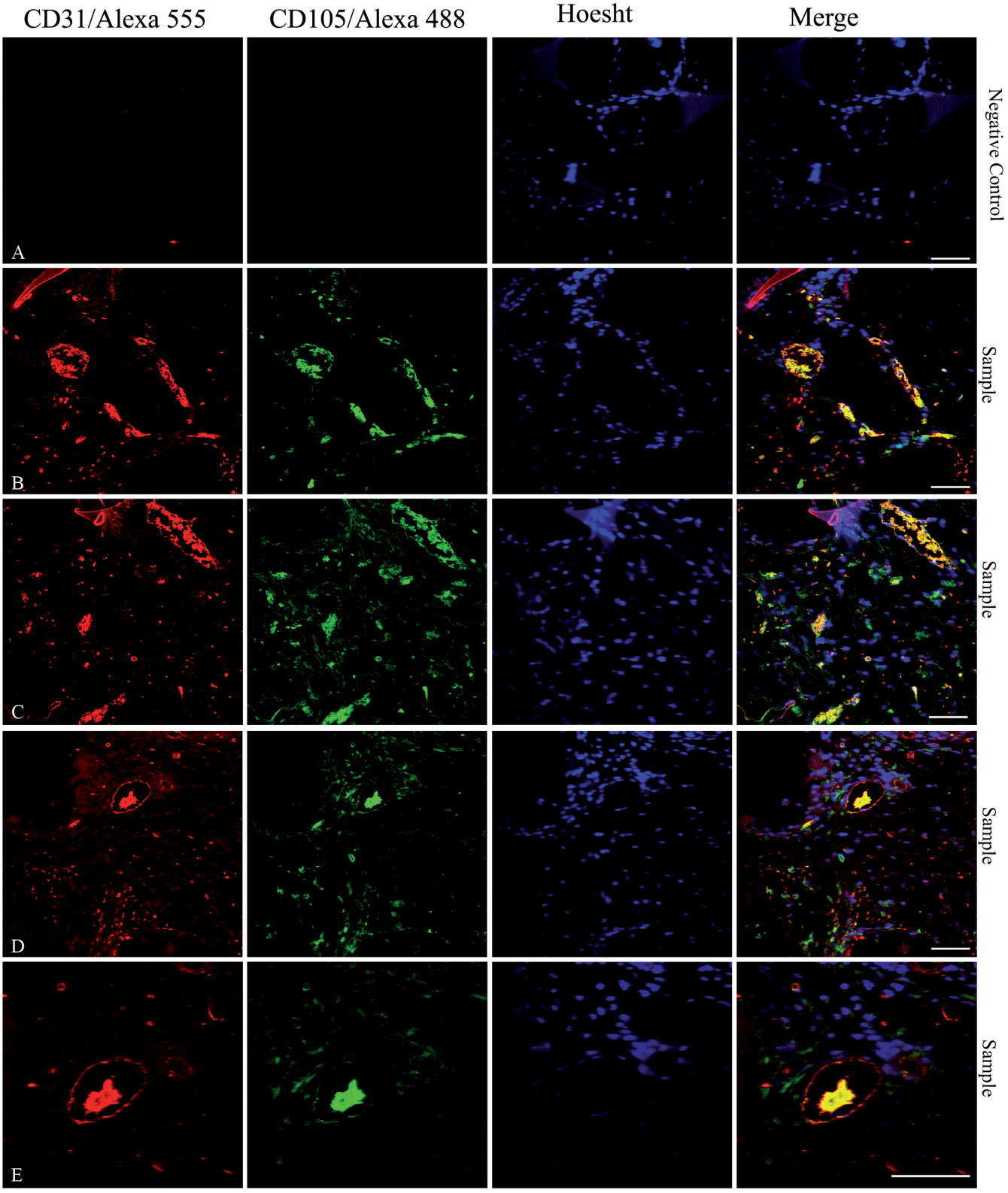

Fig. 3. Confocal micrographs of immunofluorescence CD31/CD105 double staining of 14-day old implant sections. **A.** Negative control. **B-E.** Co-localization of CD31 (conjugated with Alexa fluor 555 - red- left panels) and CD105 (conjugated with Alexa 488 - Green) blood vessel markers, and nuclear staining with Hoechst (Blue) under immunofluorescence. (**A-E**) CD31/CD 105 double stain without antigen retrieval. Observe the endothelial cells marked and the Co-Localizing signal (**B-E**). Scale bars: 50 μm.

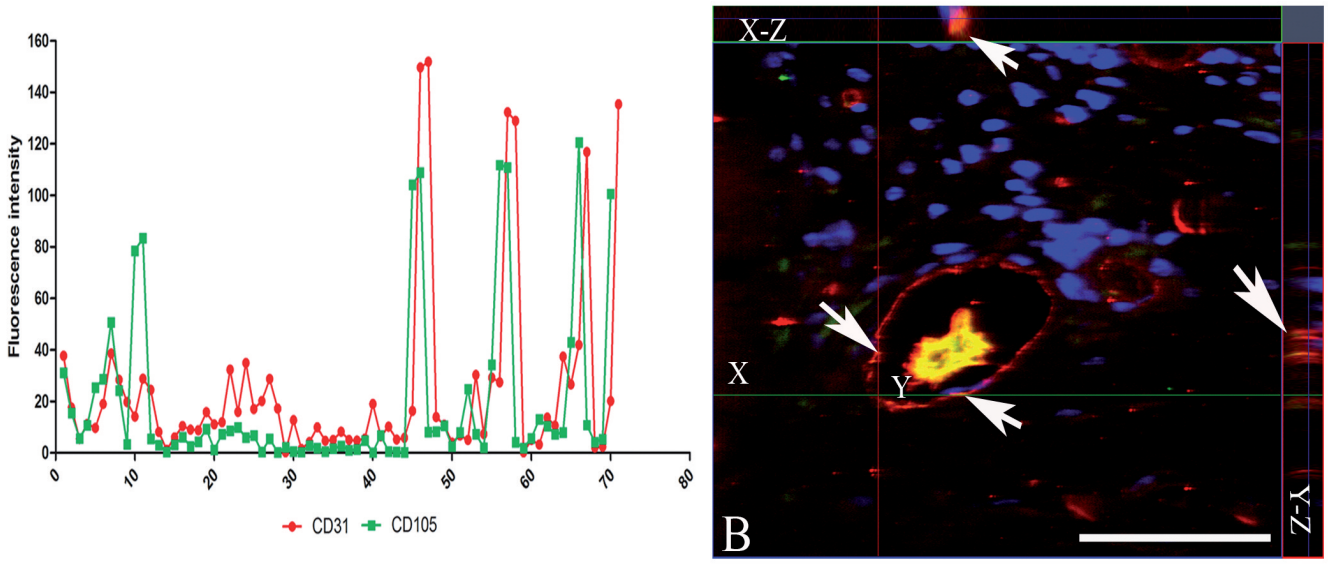

Fig. 4. Fluorescence intensity and co-localization of CD31 with CD105 in sponge implants. **A.** Fluorescence intensity by confocal Microscopy in sponges implant. **B.** Serial optical sections were collected for three-dimensional reconstruction; x-z sections are shown at the top and y-z sections are shown on the right to confirm co-localization of CD31 and CD105. The CD31 and CD105 antibodies were conjugated with secondary antibodies Alexa Fluor 555 (red) and Alexa Fluor 488 (green), respectively. Nuclear staining with Hoescht is shown in blue. The white arrows indicate endothelial cell markers that are co-located. Scale bars: 50 μm.

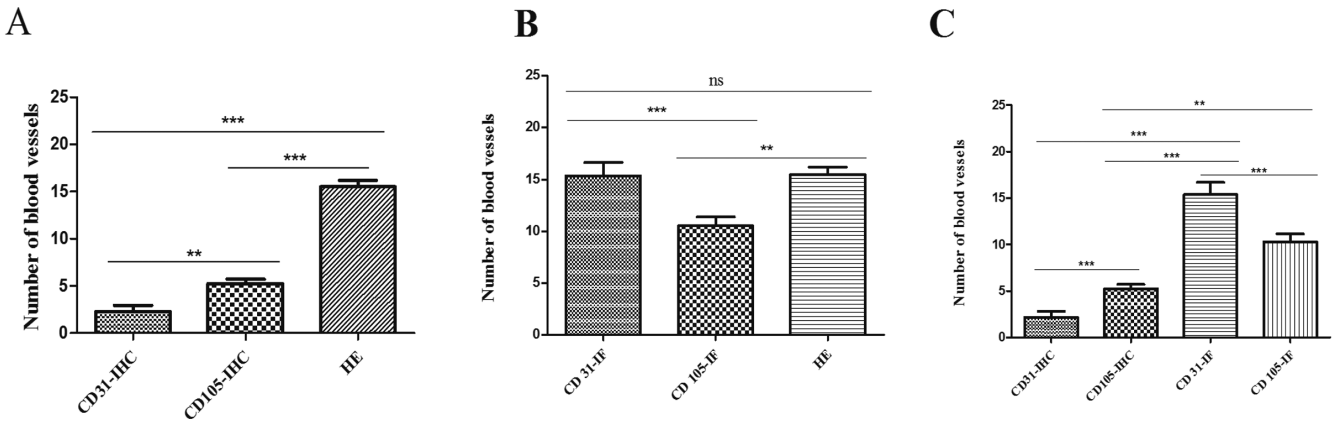

Fig. 5. Quantification of number of blood vessels. **A.** Comparative graph between number of blood vessels marked with CD31 and CD105 by IHC and number of vessels counted in HE (Hematoxylin/Eosin). **B.** Comparative graph between number of blood vessels marked with CD31 and CD105 by IF and number of vessels counted in HE (Hematoxylin/Eosin). **C.** Comparative graph between number of blood vessels marked with CD31 and CD105 by IHC and IF and number of vessels counted in HE (Hematoxylin/Eosin).

Table 3. Co-localization index.

Sample	Mean of Pearson' s Coefficient	Overlap
#1	0.35	0.79
#2	0.35	0.79
#3	0.29	0.02
#4	0.34	0.73
#5	0.24	0.74
#6	0.34	0.46
#7	0.31	0.1

Each # is the average value per animal.

morphometrically to evaluate the number of blood vessels in 14-day old implants. The mean values of the blood vessels number/field were 15±0.6 using HE staining. We observed that the number of blood vessels/field detected with immunohistochemistry was lower as compared with HE staining: 2.3±0.7 for CD31 and 5.25±0.46 for CD105 (Fig. 5A). In immunofluorescent images for CD105, the number of vessels/field detected increased to 10.5±0.8 and for CD31 the mean reached that of H&E staining (Fig. 5B).

Discussion

Successful biomaterial host integration requires the formation of functional neovascularization in and around the interface foreign body and host tissue (Andrade et al., 1987, 1996; Jones, 2006; Mendes et al, 2007; Campos et al., 2011; Pereira et al., 2012; Socarrás et al., 2014; Andrade and Ferreira, 2016). To date, none of the available techniques and/or endothelial markers employed to assess newly formed blood vessels seems to be able to highlight vascular structures convincingly. We have used a combination of immunohistochemistry and immunofluorescence techniques to identify and quantify angiogenesis in the model of subcutaneous implantation of polyether-polyurethane sponge discs in mice. This model has been used as the implanted scaffold to analyze the interaction between the host and the foreign body in rodents and to characterize the components of the fibrovascular tissue (Campos et al., 2011; Andrade and Ferreira, 2016). Immunohistochemistry, particularly in this model and in other biomaterials, has proved to be very cumbersome because of false negative results and strong background. To overcome these limitations, we compared immunohistochemistry and immunofluorescence staining for CD31 (platelet and endothelial cell adhesion molecule 1/PCAM1) and CD105 (endoglin) in subcutaneous implants of polyether-polyurethane sponge of formalin-fixed paraffin-embedded tissue. The labeling for both primary antibodies (CD31 and CD105) in IHC did not show uniformity. Some blood vessels had no labeling at all while others showed few mildly labeled endothelial cells in the same section submitted to IHC for both antibodies. Furthermore, the CD31 antibody intensity labeling was milder than the one observed for CD105 antibody. These results are in accordance with Van Amerongen et al. (2002) who observed that endothelial cell markers vWF and CD31 often failed to identify vessels in snap-frozen sections of subcutaneous implant of collagen type-1. The number of blood vessels marked with CD31 was significantly lower when compared to CD105 by immunohistochemistry. Indeed, the number of blood vessels labeled by both markers was significantly lower compared to the number of countable blood vessels in HE stained sections. These findings clearly indicate the limitation of this technique in labeling newly formed blood vessels in our implants.

With respect to IFC technique, we used double labeling for CD31 and CD105 to further analyze angiogenesis in the implants. Our results showed that labeling was homogeneous and marked more vessels, without showing a nonspecific labeling. Different antigenic retrieval methods were used. The best results for both primary antibodies CD31/CD105 were observed when no antigenic recovery was used at all.

The number of blood vessels marked with CD31 was significantly higher when compared to CD105 by immunofluorescence. Additionally, the number of blood vessels marked with CD31 using IFC showed no difference compared to the number of vessels in HE sections. In contrast, the number of blood vessels marked with CD105 using IFC was significantly lower compared to the number of vessels in HE sections. We observed positive co-localization index between CD31 and CD105, corroborating the findings of other authors that related this co-localization index with the level of blood vessel maturation (Müller et al., 2002; Newman et al.,1990; Minhajat et al., 2006; Rakocevic et al., 2017). Hence, CD105 is overexpressed in immature neoformed vessels whereas CD31 is expressed in more mature newly formed blood vessels (Newman et al., 1990; Müller et al., 2002; Minhajat et al., 2006; Rakocevic et al., 2017). These results suggest that the fourteen day implant used in this study contains mainly mature vessels. Consequently we can infer that CD31 is the best marker to be used for this blood vessel population in the implant/host interface.

We also showed that the monoclonal antibody CD31 is better because it produces less cross-reaction when compared to polyclonal antibody CD105. This may be due to the fact that CD105 is a polyclonal antibody. It is known that polyclonal antibodies bind to multiple different epitopes in a single antigen (Kim et al., 2016). Differently, the monoclonal antibodies, like CD31, recognize a single epitope in an antigen (Kim et al., 2016). This can explain why the CD105 presents cross-reactivity, which can explain the background that is observed in both techniques. However, the monoclonal antibody has some disadvantages. Due to its high specificity monoclonal antibodies need a more concentrated solution (in this study it was 1:25) compared to polyclonal ones.

In conclusion, we show that the combination of routine histology (HE staining) and IF for CD31 used in this study may provide both morphological and molecular markers for angiogenesis in implant scaffold microenvironments.

Acknowledgements: We thank FAPEMIG (Fundação de Amparo à Pesquisa do Estado de Minas Gerais) and CNPq (Conselho Nacional de Desenvolvimento Científico e Tecnológico) for the financial support and grants. We are grateful to “Centro de Aquisição e Processamento de Imagens” (CAPI- ICB/UFMG) for confocal microscopic analysis and image processing.

References

Andrade S.P. and Ferreira M.A.(2016). The sponge implant model of angiogenesis. Methods Mol. Biol. 1430, 333-343.

Andrade S.P., Fan T.P.D. and Lewis G.P. (1987). Quantitative “in vivo” studies on angiogenesis in a rat sponge model. Br. J. Exp. Pathol. 68, 755-766.

Andrade S.P., Cardoso C.C. and Machado R.D.P. (1996). Angiotensin - II- induced angiogenesis in sponge implants in mice. Int. J. Microcirc.16, 302 -307.

Campos P.P., Vasconcelos A.C., Ferreira M.A. and Andrade S.P. (2011). Alterations in the dynamics of inflammation, proliferation and

apoptosis in subcutaneous implants of lupus-prone mice. Histol. Histopathol. 26, 433-442.

Fox S.B. (2009). Assessing tumor angiogenesis in histological samples. Methods Mol. Biol. 467, 55-78.

Jones J.R. (2006). Observing cell response to biomaterials. Mater. Today 9, 34-43.

Kim S.W., Roh J. and Park C.S. (2016). Immunohistochemistry for pathologists: Protocols, pitfalls, and tips. J. Pathol. Transl. Med. 50, 411-418.

Manders E.M.M., Verbeek F.J. and Aten J.A. (1993). Measurement of co-localization of objects in dual-color confocal images. J. Microsc. 169, 375-382.

McCarthy S.A., Kuzu I., Gatter K.C. and Bicknell R. (1991). Heterogeneity of the endothelial cell and its role in organ preference of tumour metastasis. Trends Pharmacol. Sci. 12, 462-467.

Mendes J.B., Campos P.P., Ferreira M.A., Bakhle Y.S. and Andrade S.P. (2007). Host response to sponge implants differs between subcutaneous and intraperitoneal sites in mice. J. Biomed. Mater Res. B. Appl. Biomater. 83, 408-415.

Minhajat R., Mori D., Yamasaki F., Sugita Y., Satoh T. and Tokunaga O. (2006). Endoglin (CD105) expression in angiogenesis of colon cancer: analysis using tissue microarrays and comparison with other endothelial markers. Virchows Arch., 448,127-34.

Müller A.M., Hermanns M.I. and Skrzynski C. (2002). Expression of the endothelial markers PECAM-1, vWf, and CD34 in vivo and in vitro. Exp. Mol. Path. 72, 221-229.

Newman P.J., Berndt M.C. and Gorski J. (1990). PECAM-1 (CD31) cloning and relation to adhesion molecules of the immunoglobulin gene superfamily. Science 247,1219-1222.

Pereira N.B., Campos P.P., Socarrás T.J.O., Pimenta T.S., Parreiras P.M., Silva S.S., Kalapothakis E., Andrade S.P. and Moro L. (2012). Sponge implant in Swiss mice as a model for studying loxoscelism. Toxicon 59, 672-679.

Rakocevic J., Orlic D., Mitrovic-Ajtic O., Tomasevic M., Dobric M., Zlatic N., Milasinovic D., Stankovic G., Ostojić M. and Labudovic-Borovic M. (2017). Endothelial cell markers from clinician's perspective. Exp. Mol. Pathol. 102, 303-313.

Robertson D., Savage K., Reis-Filho J.S. and Isacke C.M. (2008). Multiple immunofluorescence labelling of formalin-fixed paraffin-embedded (FFPE) tissue. BMC Cell Biol. 19, 9-13.

Socarrás T.O., Vasconcelos A.C., Campos P.P., Pereira N.B., Souza J.P. and Andrade S.P. (2014). Foreign body response to subcutaneous implants in diabetic rats. PLoS One 9, e110945.

Van Amerongen M.J., Molema G., Plantinga J., Moorlag H. and Van Luyn M.J. (2002). Neovascularization and vascular markers in a foreign body reaction to subcutaneously implanted degradable biomaterial in mice. Angiogenesis 5, 173-180.

Accepted September 12, 2018